

Self-Assembled Monolayer of Short Carboxyl-Terminated Molecules Investigated with *ex Situ* Scanning Tunneling Microscopy

Cedric Dubois and Francesco Stellacci*

Department of Materials Science and Engineering, Massachusetts Institute of Technology, Cambridge, Massachusetts 02139

Received: November 27, 2007; In Final Form: February 29, 2008

Self-assembled monolayers (SAMs) of thiolated molecules have numerous potential applications and are ideal models for complex supramolecular systems. The structure of these two-dimensional crystals is not understood fully yet and deserves in-depth investigations. Here we show that a short carboxylic acid ω -terminated molecule (3-mercaptopropionic acid, MPA) forms highly ordered SAMs on Au(111) surfaces. Molecular resolution scanning tunneling microscopy (STM) images were taken at room temperature in air (*ex situ*). They showed a $\sqrt{3} \times \sqrt{3}$ unit cell that, when imaged at high set current, appears reconstructed as a $c(4 \times 2)$ superlattice. This structure is quantitatively the same as that of intermediate-length alkane thiols, but is different from the structure found previously for SAMs of the same molecule investigated with liquid-STM during the formation of the monolayer (*in situ*). This work highlights the possibility for a short ω -terminated molecule to form ordered monolayers over large areas with few defects.

Introduction

Self-assembled monolayers (SAMs) affect many of the properties of the surfaces they coat,¹ and indeed are used in fields ranging from biology^{1–4} to electronics.^{1,5,6} In most applications performance is strongly linked to the structure of the SAMs, namely the average environment of each molecule,⁷ the entropic freedom of its endgroup,² the presence of point or line defects,⁵ etc. In the last 20 years progress has been made in the characterization and understanding of SAMs' structure but not everything is understood yet.^{1,8–10} To a first approximation, medium chain length alkylthiols on Au(111) surfaces form large two-dimensional crystals that can be described with a $\sqrt{3} \times \sqrt{3}$ R30° commensurate structure, the alkyl chains being extended in an all-trans configuration, with their axes tilted about 30° with respect to the surface normal.⁸ While this description fits most experimental data, it does not fully explain some diffraction⁸ and scanning tunneling microscopy (STM) observations.¹¹ The former discrepancy has been recently solved by a few groups that have proposed the presence of gold adatoms at the sulfur plane.^{12–14} The latter is based on the fact that STM images of alkylthiol monolayers reveal a $4\sqrt{3} \times 2\sqrt{3}$ (hereafter referred as $c(4 \times 2)$) reconstruction of the $\sqrt{3} \times \sqrt{3}$ lattice.¹⁵ There are many explanations for the formation of this superlattice but none have been validated through *ab initio* calculations. Very recently Wang and Selloni were able, for the first time, to simulate through *ab initio* calculations STM images containing $c(4 \times 2)$ superlattices.¹⁶ Interestingly, to obtain their result they had to include an equilibrium population of adatoms and vacancies on the gold surfaces. In their theory the contrast between molecules observed in the $c(4 \times 2)$ superlattice is due to a difference in “contact resistance” at the gold–sulfur three-dimensional interface.

STM has been extensively used to investigate organic SAMs because it provides real-space images with unmatched subangstrom resolution, typically revealing the rich diversity of SAMs

structures.¹⁷ The interpretation of STM images is, however, not straightforward. First, images are always determined by an interplay between real surface topography and its electronic structure.¹⁸ Second, image quality is greatly affected by the cleanliness of the surface, especially in the case of hydrophilic surfaces that adsorb water from the environment. For this reason, initial imaging studies on SAMs have focused on hydrophobic molecules. Recently, research interest has shifted toward SAMs composed of molecules terminated with hydrophilic (and potentially reactive) ligand molecules (for instance carboxylic acid terminated thiolated molecules) that have great potential in biological applications³ or in the field of directed assembly.¹⁹ Structure should have an important role in these applications, for example, in determining the acid pK_a and ultimately reactivity.⁷ Recently, a $\sqrt{3} \times \sqrt{3}$ lattice has been reported for mercaptoundecanoic (MUA) molecules,²⁰ a surprising result because it implies that carboxylic acid head groups have little influence on the assembly of these molecules, despite being larger than methyl head groups and having the possibility of different types of bonding. Indeed, previous experimental works have reported a striped phase with an interline spacing of around 4.2 Å compatible with a hydrogen bond induced reconstruction.^{21,22} To further investigate this problem we decided to concentrate on a short carboxylic acid terminated molecule, mercaptopropionic acid (MPA). *In situ* STM studies of MPA SAMs showed the coexistence of 3×3 , $2\sqrt{3} \times 2\sqrt{3}$ R30°, $p \times \sqrt{3}$, and $p \times 2\sqrt{3}$ structures.^{23,24} Whether these structures are equilibrium structures also in the dry state where no exchange with solvated molecules is possible remains to be determined. To the best of our knowledge, there is no *ex situ* STM²⁵ studies on pure MPA SAMs published in the literature.

Here we report on the self-assembly of the short acid-terminated alkanethiol chain MPA. Molecular resolution STM investigation reveals large areas of densely packed monolayer in a $\sqrt{3} \times \sqrt{3}$ surface reconstruction displaying a $c(4 \times 2)$ superlattice similar to what is routinely observed on methyl-terminated alkanethiols.^{9,17} The large monophased areas are

* Corresponding author. E-mail: frstell@mit.edu.

delimited by regions displaying stripes. We strikingly observe the absence of etch pits in our images in contrast to alkanethiols SAMs prepared under the same conditions. We demonstrate that short carboxylic alkanethiol chains can form highly ordered SAMs on Au(111). In addition, we observe a reproducible smooth contrast transition from the $c(4 \times 2)$ superlattice to a $\sqrt{3} \times \sqrt{3}$ structure with decreasing tunnel current, which could be explained by different decay lengths parallel to the surface normal for the wave functions of the nonequivalent molecules in the unit cell. In addition to contributing to the understanding of the alkanethiol SAM formation, these findings are relevant for the functionalization of organic surfaces.

Experimental Section

Flame annealed Au(111) on mica purchased from Molecular Imaging and Phasis SARL were used as substrates. 3-Mercaptopropionic acid and 11-mercaptoundecanoic acid were purchased from Alfa Aesar and used as received.

We used a Digital Instruments Multimode Nanoscope IIIa (with both E and A scanners)²⁶ installed in an acoustic chamber mounted on a vibration damping system. All the measurements were performed at room temperature in air with constant current mode. We used platinum–iridium STM tips either mechanically cut or chemically etched, both techniques giving identical images. The STM measurements, reproducible over the time scale of our experiments (several months), show that our samples did not suffer from surface contamination or aging effects. Our results on MPA were consistently obtained on 8 samples using tens of tips. Molecular resolution has been achieved in a wide parameter window: the bias voltage (applied to the sample) and tunnel current used ranged from $V_b = \pm 300$ –900 mV and $I_t = 25$ –800 pA, respectively, with the precise values explicitly mentioned with each image. The images acquired at low voltages, $V_b \leq 300$ mV ($I_t = 500$ pA), still show molecular resolution but are of poor definition. Similarly, a reversible image degradation occurs when the tunnel current is increased above 1 nA ($V_b = 500$ mV). The likely explanation is a perturbation of the SAM head groups due to the too close proximity of the STM tip. Since our measurements have been performed in air at room temperature, some of our images exhibited a distortion due to thermal drift. We have therefore, after identifying the drift direction and velocity by scanning at different tip speeds, treated these images to correct for the drift (mentioned in the captions). Prior to the investigation of the SAMs we carefully selected all the tips by achieving atomic resolution on highly oriented pyrolytic graphite.

Results and Discussion

To investigate monolayers of carboxylic acid ω -terminated thiolated molecules on gold surfaces we first prepared and investigated well-established alkyl-thiol SAMs. We focused on butanethiol, hexanethiol, octanethiol, and dodecanethiol monolayers. We prepared these monolayers by immersing our gold substrates in 1 mM solutions with toluene or ethanol for periods of time varying from 1 day to 1 week. After removal from solution, the samples were dried in air sometimes after rinsing in the same solvent. To the best of our observations we found no difference in the final structure of the SAMs as a function of the assembly time, the molecules used, or the solvent. In all cases we observed phases rich in etch pits similar to what is observed in literature.¹⁰ We did not investigate these SAMs thoroughly but used them only as a metric of comparison relative to other published results and to the carboxylic acid terminated SAMs that we assembled in the exact same conditions. When

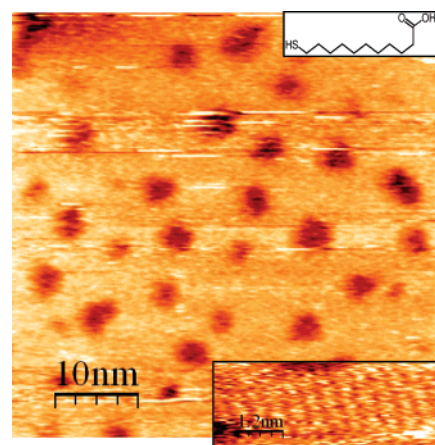


Figure 1. Ex-situ STM topographies showing 11-mercaptoundecanoic acid (MUA, schematic in the inset) SAMs covering Au(111). Lower inset: Isolated region displaying crystallization. ($V_b = 800$ mV, $I_t = 25$ pA.)

we studied 11 mercaptoundecanoic acid (MUA) SAMs assembled from toluene and ethanol solutions for periods of times ranging from 1 day to 1 week we observed a somewhat different behavior. Also in the case of these SAMs there was no observable morphological difference as a function of assembly time and solvent and all SAMs were rich in etch pits. Molecular resolution could not be achieved (Figure 1), we seldom observed isolated regions with a $\sqrt{3} \times \sqrt{3}$ unit cell (Figure 1 lower inset), similar to what has been reported in the literature.²⁰ On the basis of these observations it is reasonable to suspect that in the assembly conditions used, MUA forms “amorphous” SAMs, that is, containing only short-range order. The lack of molecular resolution on these SAMs could be ascribed to the adsorption of a water layer or other hydrophilic contaminants from air or solution, but the results presented below on MPA SAM question this common belief.

Different results were obtained when assembling MPA monolayers. When the SAMs were prepared from ethanol we observed morphologies similar to those described for MUA monolayers, i.e., etch pit-rich “amorphous” layers even after 1 week of assembly time. In the case of SAMs obtained from toluene solutions, already after 1 day highly ordered etch pit-free layers were routinely observed. It should be noticed that the presence of etch pits in the “ethanol” SAMs versus their absence in their “toluene” counterparts is an indication that these SAMs are morphologically different, as opposed to the “ethanol” SAMs being similar to the “toluene” ones but covered by some impurity. Figure 2a shows a representative image of a MPA SAM assembled from a toluene solution, containing a relatively large single crystal with boundaries constituted of a striped $11 \times \sqrt{3}$ phase (flat lying phase). Figure 2b shows the same SAM assembled from ethanol. We believe that these results highlight the effect of solvent on the morphology of a SAM. It is reasonable to expect that SAMs prepared from toluene (where MPA is less soluble compared to ethanol) could reach equilibrium faster when compared to ethanol-derived SAMs, yet even after 1 week we saw no hint of the etch pit-free morphology observed after 1 day in toluene.

Next we focused on the highly ordered phase that we observed on all our MPA SAMs formed from toluene. As shown in Figure 3, molecular resolution STM reveals a $\sqrt{3} \times \sqrt{3}$ structure with a $c(4 \times 2)$ superlattice reminiscent of the extensively studied alkanethiols. The carboxyl-terminated head group of MPA, although larger than the alkanethiol molecule, is sufficiently small (carboxyl–carbonyl oxygen distance = 2.2 Å) to conform in this lattice. This is reasonable if one compares

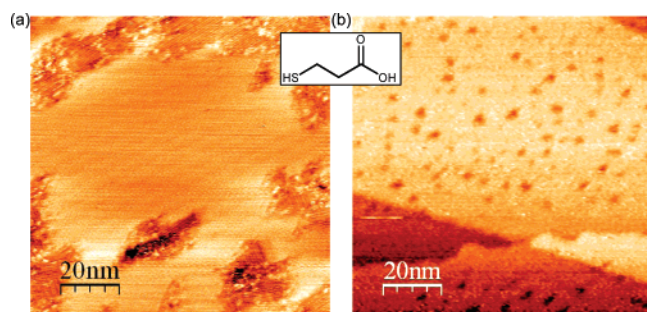


Figure 2. Ex situ STM topographies of MPA (schematic in the inset) SAMs formed from toluene (a) and ethanol (b) solutions. (a) Etch pit-free MPA highly ordered domain delimited by regions displaying a striped phase. (b) Etch pits rich amorphous MPA monolayer formed in ethanol. ($V_b = 500$ mV, $I_t = 500$ pA.) All the images presented in this paper (raw data) have been postprocessed using WsXM software (with slope correction and linear interpolation between pixels but without FFT filtering).³⁵

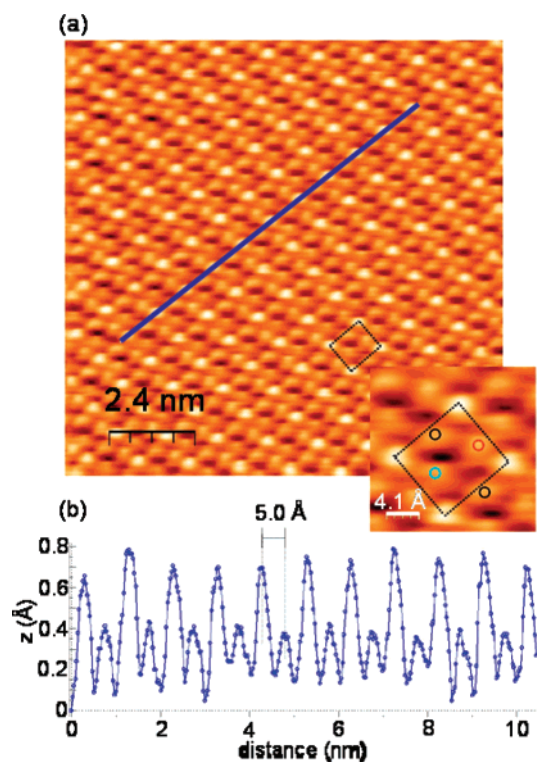


Figure 3. (a) STM molecular resolution image showing the $c(4 \times 2)$ structure together with the $3 \times 2\sqrt{3}$ unit cell. Inset: Zoom into the unit cell (rectangle) with the positions of the nonequivalent molecules. (b) Height profile running along the blue line in (a) crossing the corner molecules. ($V_b = 500$ mV, $I_t = 500$ pA.)

these SAMs with benzyl mercaptan SAMs, where the constituent molecules comprise a larger diameter (benzene ring outer diameter = 2.8 Å) than MPA molecules, but also self-assemble into a regular $\sqrt{3} \times \sqrt{3}$ R30° lattice.^{10,27} It also seems to exclude any substantial enthalpic contribution to the SAM formation from head group interactions (such as H-bonds or van der Waals types of interactions). As shown by the line profile (Figure 3b) taken across the brightest molecules, the average molecular spacing is 5.0 ± 0.1 Å. The inset of Figure 3a displays one rectangular unit cell (chosen as $3 \times 2\sqrt{3}$) together with the locations of the molecules observed with STM. We observe that the positions of the molecules slightly deviate from a perfectly hexagonal $\sqrt{3} \times \sqrt{3}$ lattice. The molecules marked by black circles are clearly off the dotted line of the

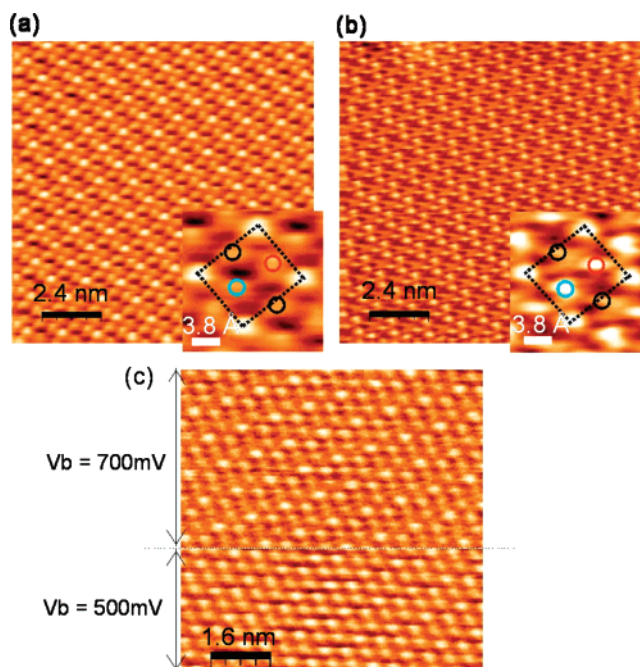


Figure 4. Different contrasts for the molecules in the $c(4 \times 2)$ structure have been observed at different locations on our sample: (a) β -contrast and (b) ζ -contrast following Ripsan et al.¹⁷ ($V_b = 500$ mV, $I_t = 500$ pA.) (c) Images acquired switching from $V_b = 500$ to 700 mV ($I_t = 500$ pA) while scanning showing the continuity of the structure. (Panels b and c were drift-corrected.)

unit cell. This phenomenon, also observed for alkanethiols, has yet to be fully explained.²⁸

It is known that STM images of SAMs showing $c(4 \times 2)$ reconstructions show different “polymorphs” of the unit cells where the relative intensity of the atoms changes.¹⁷ We observed the same phenomenon on our SAMs—specifically, we observed one polymorph per single crystal, but we could observe several polymorphs on the same substrate while keeping all of the imaging parameters the same. Two different polymorphs are shown in Figure 4 as an example. In Figure 4a the brightest molecules are the four molecules standing at the corner of the unit cell, in Figure 4b the brightest molecules are in a coupled staircase arrangement. The reproducibility of these topographies after successive scans has also demonstrated the stability of the domains with respect to the STM probe, thus ruling out the possibility of tip-induced rearrangements of the molecules. We also note that we did not observe the presence of different polymorphs in the same STM image as previously observed by Ripsan et al. on undecanethiol SAMs.¹⁷ At present we believe that we did not succeed to image boundaries between polymorphs due to the large size of our single crystals. Further work needs to be performed to clarify this point.

With the aim of probing whether these observed polymorphic structures are straightforward effects of the spatial variation of the local density of states (LDOS) we have acquired images at several bias voltages and tunnel currents (set points). Scanning the same area at different bias voltage from $V_b = 500$ to 900 mV (probing the unoccupied states) only slightly modify the relative brightness of the molecules in the unit cell. However, due to a slow but not negligible thermal drift it is difficult to locate the same atom in two successive images. We have thus made certain that the molecules in the unit cell do not exchange their brightness between images acquired at different voltage and current set points. As shown in Figure 4c, the continuity of the structure between the lower and upper parts of the topography (the voltage was switched from 500 mV to 700 mV

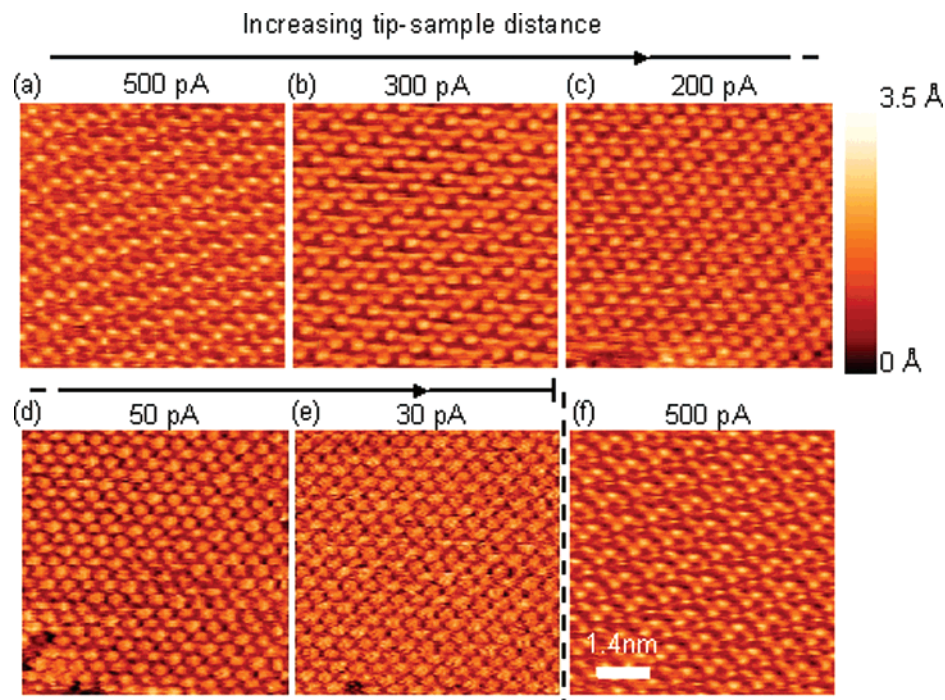


Figure 5. (a–e) Series of images ($7 \times 7 \text{ nm}^2$) acquired at the same location with tunnel currents in the range $I_t = 500\text{--}30 \text{ pA}$ showing a transition of the molecule contrast. (f) Image acquired after changing back the current showing the reversibility of the transition ($I_t = 500 \text{ pA}$). The z -scale (color-scale) is kept constant. ($V_b = 500 \text{ mV}$ for all images.)

while scanning) allowed us to observe that the brightest spots correspond to equivalent molecules in both structures. This suggests that within our imaging range the polymorphic structures observed are linked to the monolayer structure rather than to some electronic imaging effect.

Finally, we investigated the LDOS z -dependence by varying the tunnel current from 500 to 30 pA. As shown in Figure 5, we observe a transition in the contrast of our images from a clear $c(4 \times 2)$ at 500 pA to what appears a $\sqrt{3} \times \sqrt{3}$ structure at 30 pA. Image appearance (and quality) did not depend on the sequence of currents used. It should be noted that the images shown are all on the same color scale, hence the contrast obtained *per molecule* remained constant as the tip was retracting (smaller current); the only things that changed were the intensity ratio between molecules and the apparent size of the molecules. The strong contrast between the molecules in the unit cell occurs when the tip probes the LDOS closer to the SAM whereas no contrast between molecules is observed farther from the SAM. An irreversible tip-induced $\sqrt{3} \times \sqrt{3}$ to $c(4 \times 2)$ rearrangement of the structure of decanethiolate SAMs on Au(111) has been reported in the literature.²⁹ However, in our case, the reversible contrast transition renders a tip-induced scenario very unlikely. Another study of butanethiol and dodecanethiol has reported reversible $\sqrt{3} \times \sqrt{3} \rightleftharpoons c(4 \times 2)$ structural fluctuations under the same tip and voltage conditions.³⁰ We point out that, at a given current–voltage setpoint in our experiments, the targeted areas have always displayed the same polymorph during each measurement (time scale typically $\sim 1 \text{ h}$). The origin of this contrast transition calls for further investigations. However, since STM in the constant current mode maps isosurfaces of the LDOS, such a contrast transition could be qualitatively explained considering different decay lengths of the wave functions for the nonequivalent molecules assuming these latter are standing at slightly different physical heights (z -position), resulting from either different sulfur adsorption sites or the presence of adatoms.¹⁶ In any case, we think this contrast transition worth

reporting and believe that spectroscopic measurements would provide a more conclusive answer.

Conclusions

Our results show that short carboxylic-terminated molecules self-assemble onto Au(111) forming a $\sqrt{3} \times \sqrt{3}$ structure featuring a $c(4 \times 2)$ superlattice similar to the well-known alkanethiol case. In addition, the absence of etch pits demonstrates the possibility for short alkyl chains to form a long-range ($\sim 100 \text{ nm}$) ordered monolayer. Finally, our results on MPA SAMs on flat surfaces should form a basis for a deeper understanding of STM observations of mixed monolayers containing MPA molecules, specifically in the case of SAMs on nanoparticles,^{1,31,32} a topic that our group has been studying in recent years.^{33,34}

Acknowledgment. The authors thank G. Heimel for valuable discussions. C.D. acknowledges support from the Swiss National Science Foundation. F.S. acknowledges the Packard Foundation and the NSF CAREER (DMR 06-45323) awards.

References and Notes

- (1) Love, J. C.; Estroff, L. A.; Kriebel, J. K.; Nuzzo, R. G.; Whitesides, G. M. *Chem. Rev.* **2005**, *105*, 1103.
- (2) Lahann, J.; Mitragotri, S.; Tran, T. N.; Kaido, H.; Sundaram, J.; Choi, I. S.; Hoffer, S.; Somorjai, G. A.; Langer, R. *Science* **2003**, *299*, 371.
- (3) Mrksich, M. *Chem. Soc. Rev.* **2000**, *29*, 267.
- (4) Mrksich, M.; Whitesides, G. M. *Annu. Rev. Biophys. Biomol. Struct.* **1996**, *25*, 55.
- (5) Halik, M.; Klauk, H.; Zschieschang, U.; Schmid, G.; Dehm, C.; Schutz, M.; Maisch, S.; Effenberger, F.; Brunnbauer, M.; Stellacci, F. *Nature* **2004**, *431*, 963.
- (6) Kim, C.; Facchetti, A.; Marks, T. J. *Science* **2007**, *318*, 76.
- (7) Creager, S. E.; Clarke, J. *Langmuir* **1994**, *10*, 3675.
- (8) Schreiber, F. *Prog. Surf. Sci.* **2000**, *65*, 151.
- (9) Poirier, G. E. *Chem. Rev.* **1997**, *97*, 1117.
- (10) Yang, G. H.; Liu, G. Y. *J. Phys. Chem. B* **2003**, *107*, 8746.
- (11) Poirier, G. E.; Tarlov, M. J. *Langmuir* **1994**, *10*, 2853.

- (12) Maksymovych, P.; Sorescu, D. C.; Yates, J. T. *Phys. Rev. Lett.* **2006**, *97*, 146103.
- (13) Mazzarello, R.; Cossaro, A.; Verdini, A.; Rousseau, R.; Casalis, L.; Danisman, M. F.; Floreano, L.; Scandolo, S.; Morgante, A.; Scoles, G. *Phys. Rev. Lett.* **2007**, *98*, 016102.
- (14) Yu, M.; Bovet, N.; Satterley, C. J.; Bengio, S.; Lovelock, K. R. J.; Milligan, P. K.; Jones, R. G.; Woodruff, D. P.; Dhanak, V. *Phys. Rev. Lett.* **2006**, *97*.
- (15) The historical $c(4 \times 2)$ notation of the superlattice is based on a hexagonal coordinate system. Another commonly used notation is based on the rectangular structure and is written $(3 \times 2\sqrt{3})$.
- (16) Wang, J. G.; Selloni, A. *J. Phys. Chem. C* **2007**, *111*, 12149.
- (17) Riposan, A.; Liu, G.-y. *J. Phys. Chem. B* **2006**, *110*, 23926.
- (18) Bumm, L. A.; Arnold, J. J.; Dunbar, T. D.; Allara, D. L.; Weiss, P. S. *J. Phys. Chem. B* **1999**, *103*, 8122.
- (19) Barsotti, R. J.; Stellacci, F. *J. Mater. Chem.* **2006**, *16*, 962.
- (20) Mendoza, S. M.; Arfaoui, I.; Zanarini, S.; Paolucci, F.; Rudolf, P. *Langmuir* **2007**, *23*, 582.
- (21) Sprik, M.; Delamarche, E.; Michel, B.; Rothlisberger, U.; Klein, M. L.; Wolf, H.; Ringsdorf, H. *Langmuir* **1994**, *10*, 4116.
- (22) Gorman, C. B.; He, Y. F.; Carroll, R. L. *Langmuir* **2001**, *17*, 5324.
- (23) Sawaguchi, T.; Sato, Y.; Mizutani, F. *Phys. Chem. Chem. Phys.* **2001**, *3*, 3399.
- (24) Esplandiù, M. J.; Hagenstrom, H.; Kolb, D. M. *Langmuir* **2001**, *17*, 828.
- (25) Ex situ STM refers to STM operated in air as opposed to in situ STM which refers to STM performed in a liquid cell.
- (26) The E and A scanners possess different bulk geometries, approach mechanisms, and scanning ranges (7.6 and 0.7 μm respectively). We have used the E scanner to acquire larger scale images of our samples while using the A scanner to obtain more accurate measurements at smaller scale. We have found the latter more stable with respect to mechanical noise.
- (27) Tao, Y. T.; Wu, C. C.; Eu, J. Y.; Lin, W. L.; Wu, K. C.; Chen, C. H. *Langmuir* **1997**, *13*, 4018.
- (28) Zeng, C. G.; Li, B.; Wang, B.; Wang, H. Q.; Wang, K. D.; Yang, J. L.; Hou, J. G.; Zhu, Q. S. *J. Chem. Phys.* **2002**, *117*, 851.
- (29) Touzov, I.; Gorman, C. B. *J. Phys. Chem. B* **1997**, *101*, 5263.
- (30) Teran-Arce, F.; Vela, M. E.; Salvarezza, R. C.; Arvia, A. J. *Langmuir* **1998**, *14*, 7203.
- (31) Templeton, A. C.; Wuelfing, M. P.; Murray, R. W. *Acc. Chem. Res.* **2000**, *33*, 27.
- (32) Daniel, M.-C.; Astruc, D. *Chem. Rev.* **2004**, *104*, 293.
- (33) Jackson, A. M.; Myerson, J. W.; Stellacci, F. *Nat. Mater.* **2004**, *3*, 330.
- (34) Jackson, A. M.; Hu, Y.; Silva, P. J.; Stellacci, F. *J. Am. Chem. Soc.* **2006**, *128*, 11135.
- (35) Horcas, I.; Fernandez, R.; Gomez-Rodriguez, J. M.; Colchero, J.; Herrero, J. G.; Baro, A. M. *Rev. Sci. Instrum.* **2007**, *78*, 013705.